X-525-68-428

NASA TM X- 63401

COMPUTED RADIATION PATTERNS OF A THERMALLY DISTORTED 30-FOOT ATS F AND G PARABOLIC REFLECTOR ANTENNA

RICHARD F. SCHMIDT

NOVEMBER 1968

GSFC

GODDARD SPACE FLIGHT CENTER
GREENBELT, MARYLAND

X-525-68-428

COMPUTED RADIATION PATTERNS OF A THERMALLY DISTORTED 30-FOOT ATS F AND G PARABOLIC REFLECTOR ANTENNA

Richard F. Schmidt

November 1968

GODDARD SPACE FLIGHT CENTER
Greenbelt, Maryland

COMPUTED RADIATION PATTERNS OF A THERMALLY DISTORTED 30-FOOT ATS F AND G PARABOLIC REFLECTOR ANTENNA

Richard F. Schmidt
Advanced Development Division

ABSTRACT

Far-field radiation patterns of a thermally distorted ATS F and G 30-foot antenna are computed at 2 GHz and 8 GHz by an IBM 360 Mod. 91 computer using a second-order polynomial representation of the antenna surface. Radiation patterns of the undistorted reflector are included to establish a basis for comparison, and the effect of improper feed positioning is investigated.

PRECEDING PAGE BLANK NOT FILMED.

CONTENTS

ILLUSTRATIONS

GLOSSARY OF NOTATIONS

Symbol	Meaning
δ	displacement, or increment
$\bar{n}$	surface normal
F	focal length
D	diameter
$\bar{E}_\theta$, $\bar{E}_\phi$	vector electric fields
Z_1	vertex displacement
FRC	sampling on surface of integration
λ	wavelength
f	frequency
α, β, γ	Euler angles for feed rotation
x_ϵ, y_ϵ, z_ϵ	scalar components of vector feed displacement $\bar{\rho}_\epsilon$
R_1	radius of sphere of observation
N	exponent of prime feed pattern, $\mathfrak{I}_1 = \cos^N \Theta$
σ_0, $\sigma_{max.}$	minimum and maximum radii of antenna surface
θ, ϕ	coordinate angles of observer
Θ, Φ	coordinate angles at surface
g	gravitational constant
ψ_θ, ψ_ϕ	phase angles of $\bar{E}_\theta$, $\bar{E}_\phi$
m	polynomial order
a_i	polynomial coefficients
K	beam deviation factor
Δ	lateral feed displacement

COMPUTED RADIATION PATTERNS OF A THERMALLY DISTORTED 30-FOOT ATS F AND G PARABOLIC REFLECTOR ANTENNA

INTRODUCTION

A modular computer program based on the vector Kirchhoff theory of diffraction, and written in Fortran IV, has been used by the Antenna Systems Branch of the Advanced Development Division at Goddard Space Flight Center to compute antenna radiation patterns for the Applications Technology Satellite and other space projects (References 1 and 2). The antenna parameters of the ATS 30-foot reflector include wavelength, feed orientation angles, feed displacement components, range, source polarization, minimum and maximum reflector radii, and surface coordinate data. Computations were made at the request of the Systems Division.

SURFACE DISTORTION

All antenna parameters were utilized directly by the existing program with the exception of the surface coordinate data resulting from the thermal gradient across the deployed reflector. Figure 1 shows the thermal gradient and the corresponding surface displacements along the normals to the original paraboloid.

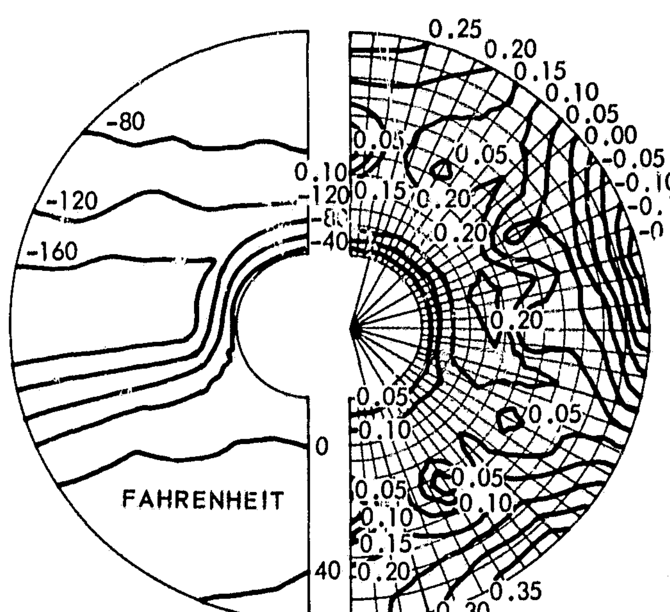

Figure 1—Thermal gradient and surface distortion of 30-foot ATS reflector.

A new subroutine, capable of fitting a least-squares polynomial to the surface coordinate data, was annexed to the modular program and verified by utilizing the coordinates for the undistorted reflector without a central hole. Comparison of the radiation patterns obtained from this ideal paraboloidal surface with approximation formulas for obtaining beam width, side-lobe level, and first null position showed good agreement. About 400 coordinate triplets (x, y, z) were then taken from the surface of the distorted ATS antenna and supplied to the computer as input to generate a polynomial surface description.

Polynomial order 2 was utilized for this slightly distorted quadric surface although order 5 has been implemented in the program. The surface data, fitted to the equation

$$z = a_0 + a_1 y + a_2 y^2 + a_3 x + a_4 xy + a_5 x^2$$

yielded the following coefficients.

$a_0 = -13.19149,$	$a_1 = 0.00002,$	$a_2 = 0.01891$
$a_3 = -0.00036,$	$a_4 = 0.00000,$	$a_5 = 0.01902$

The slight distortion due to thermal effects on the reflector is exhibited by the small values of the coefficients a_1, a_3, and a_4. If these were all identically zero, the polynomial would reduce to

$$z = -13.19 + 0.019\, y^2 + 0.019\, x^2$$

This is recognized as the equation of an elliptic paraboloid

$$\frac{x^2}{a^2} + \frac{y^2}{b^2} = z$$

when $a = b$ (paraboloid of revolution) and the vertex is displaced from the origin of coordinates by an amount $Z_1 = -F = -13.2$ feet. From the parametric representation of a paraboloid,

$$x = \sigma \sin \zeta, \qquad y = -\sigma \cos \zeta, \qquad z = \frac{\sigma^2}{4F} + z_1$$

it follows that $1/a^2 = 1/4F = 0.019$ for the present case, and this agrees with the values a_2 and a_5 found by the computer. Therefore, the complete set of coefficients (a_i) represents a nearly-quadric surface. The RMS deviation between the input data and the polynomial surface was computed as 0.00650 ft.

The polynomial surface description allows computation of surface normals, differential areas, etc. in complete analogy with analytical formulations such as the parametric representation shown above. Adequate sampling was obtained for the diffraction integral by resolving the reflector surface into approximately 4000 and 60,000 differential areas at 2 GHz and 8 GHz, respectively. Computer running time for a pattern cut is not significantly increased by formation of the surface polynomial. Polynomial coefficients a_i are found only once, for a given surface condition, to establish the illumination on the reflector. The integration over the antenna surface is inherently far more time-consuming and is repeated for every field point.

RADIATION PATTERNS (2 GHz, 8 GHz)

In both the 2 GHz and 8 GHz cases reference patterns were computed for an undistorted paraboloid with a central hole of 3.5-foot radius, consistent with Figure 1. It can be seen from Figures 2 and 4 that the phase transitions for these reference patterns are π-radian jump discontinuities at the pattern nulls. Cross-polarized energies, given as E_ϕ, are lower than -90 db and -75 db at 2 and 8 GHz, respectively, and are therefore, relatively insignificant. The broadening of the first sidelobe of the E_θ pattern is due to the hole in the center of the antenna. A slight narrowing of the width of the main beam of the E_θ pattern is also in evidence.

At 2 GHz the effect of the thermal distortions given in Figure 1 is slight. See Figure 3. It is recalled that the distortions ranged from -0.20 inch to +0.35 inch and should be related to a free-space wavelength of 5.9 inches at 2 GHz. Figure 3 shows that the phase transitions at pattern nulls are still approximately π radians, but are now continuous transitions rather than jump discontinuities. It is noted that pattern minima (instead of nulls) do not exhibit the characteristic π radian changes. Cross-polarized energy E_ϕ has increased by more than 60 db at $\phi = 0$, but remains about 25 db below the principal polarization E_θ. Main-lobe beamwidth is not greatly affected by the thermal distortion.

At 8 GHz the effect of the same set of thermal distortions is much greater and the -0.20 inch to +0.35 inch displacements should be related to a free space wavelength of only 1.47 inch. Figure 5 shows very gradual phase transitions and null-filling in the radiation patterns. The first "null" in the E_θ pattern has become a "minimum" of about -18 db depth relative to the maximum energy level. The first side-lobe level is also higher by approximately 4 db, and the width of the main beam has increased slightly. Cross-polarized energy levels are not much higher than at 2 GHz. It appears that the distortions at 8 GHz degrade the antenna somewhat, but the reflector is still useful.

FEED DISPLACEMENT (2 GHz, 8 GHz)

The mathematical model of the radiating antenna system is made more exact when the sphere of uncertainty for feed positioning is included. In the present problem, the sphere of uncertainty reduced to a line of uncertainty. Information supplied by the Systems Division set the bound of uncertainty for prime-feed phase center positioning at $y_f = \pm 0.03075$ foot, or $\lambda/16$, at 2 GHz. Figure 6 shows the result of the computation which now includes: a central hole of 7-foot diameter in the main reflector, the thermal distortions of Figure 1, and a lateral feed displacement of $\lambda/16$ without rotation. It can be seen that the lateral feed displacement causes a slight displacement of the radiation pattern in space (scanning) in the opposite direction. Comparison with the approximation formula for estimating the scan angle,

$$\theta_s \approx \sin^{-1} \frac{K\Delta}{F} ,$$

is satisfactory as θ_s is approximately 0.12° by the equation and 0.10° by the computer via the diffraction integral. The approximation formula ignores the illumination taper on the antenna surface.

At 8 GHz the effect of a fixed 0.03075-foot mechanical displacement of the feed produces a significant amount of scanning of the main beam. Figure 7 shows the result of the computation which includes the central 7-foot hole in the main reflector, the thermal distortions of Figure 1, and a $\lambda/4$ lateral feed displacement at 8 GHz. The scan angle θ_s is computed approximately equal to 0.107°, and compares with 0.11° taken from the computer plot.

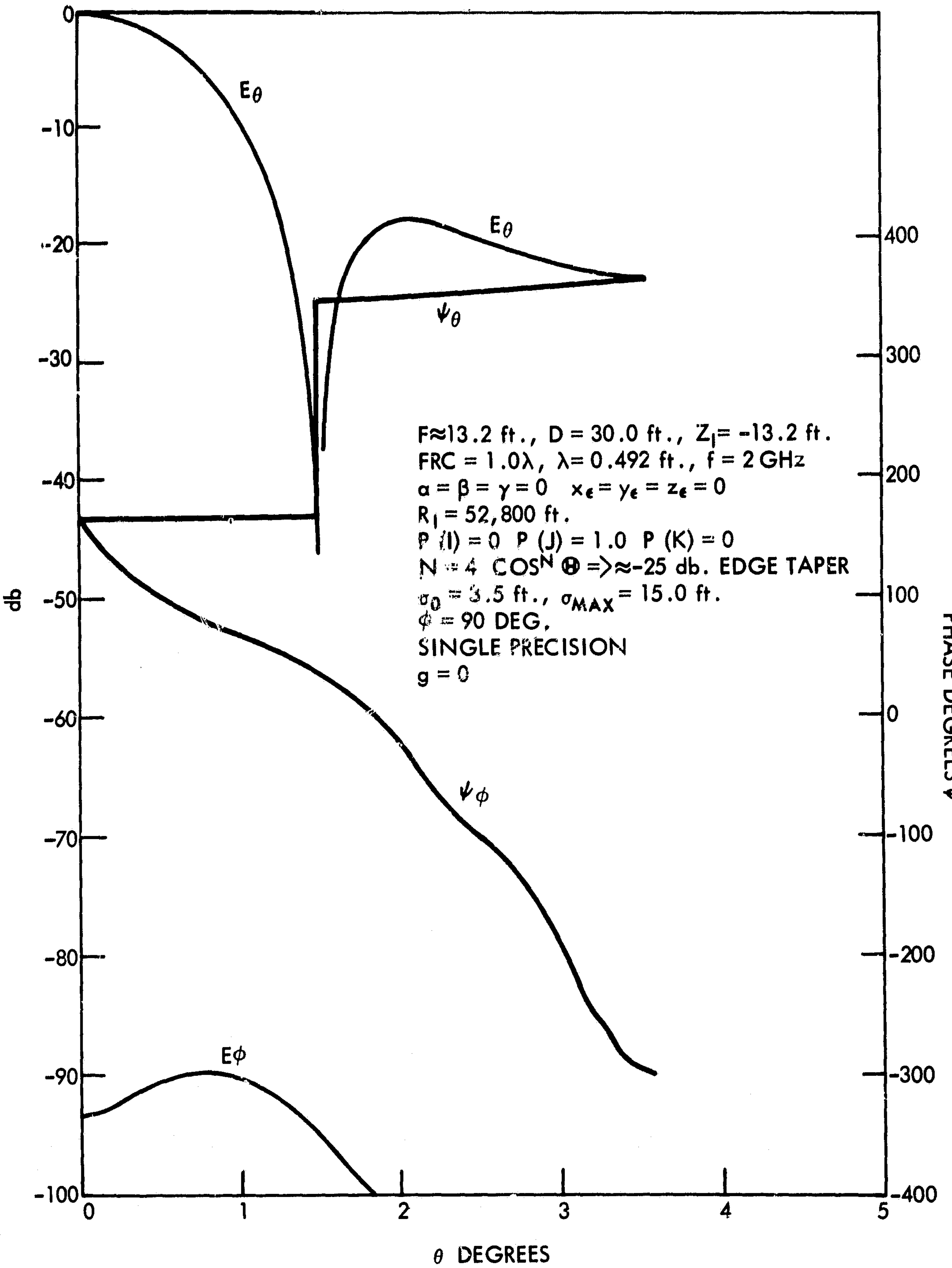

Figure 2–ATS paraboloid without thermal distortion (2 GHz).

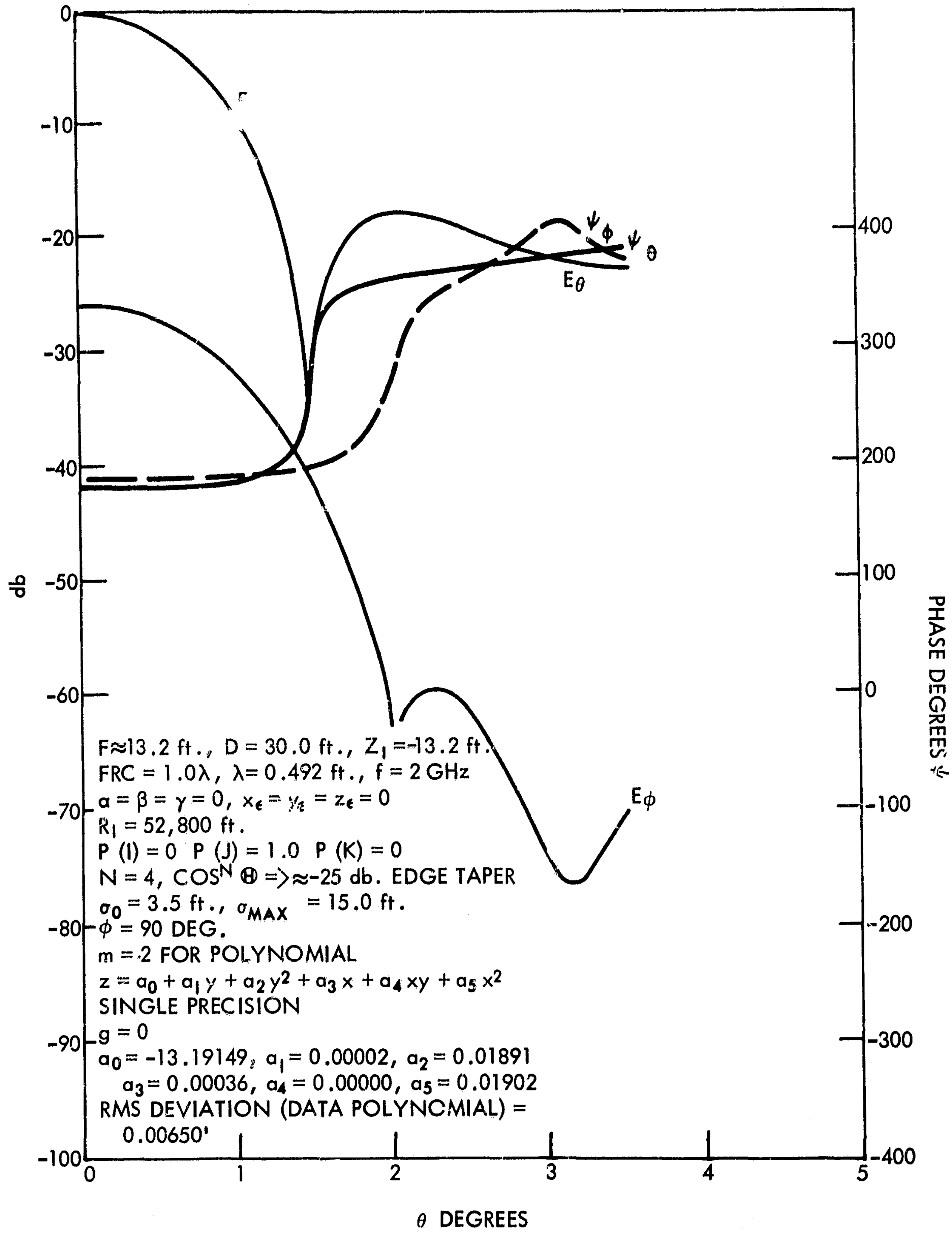

Figure 3–Paraboloid with thermal distortion (2 GHz).

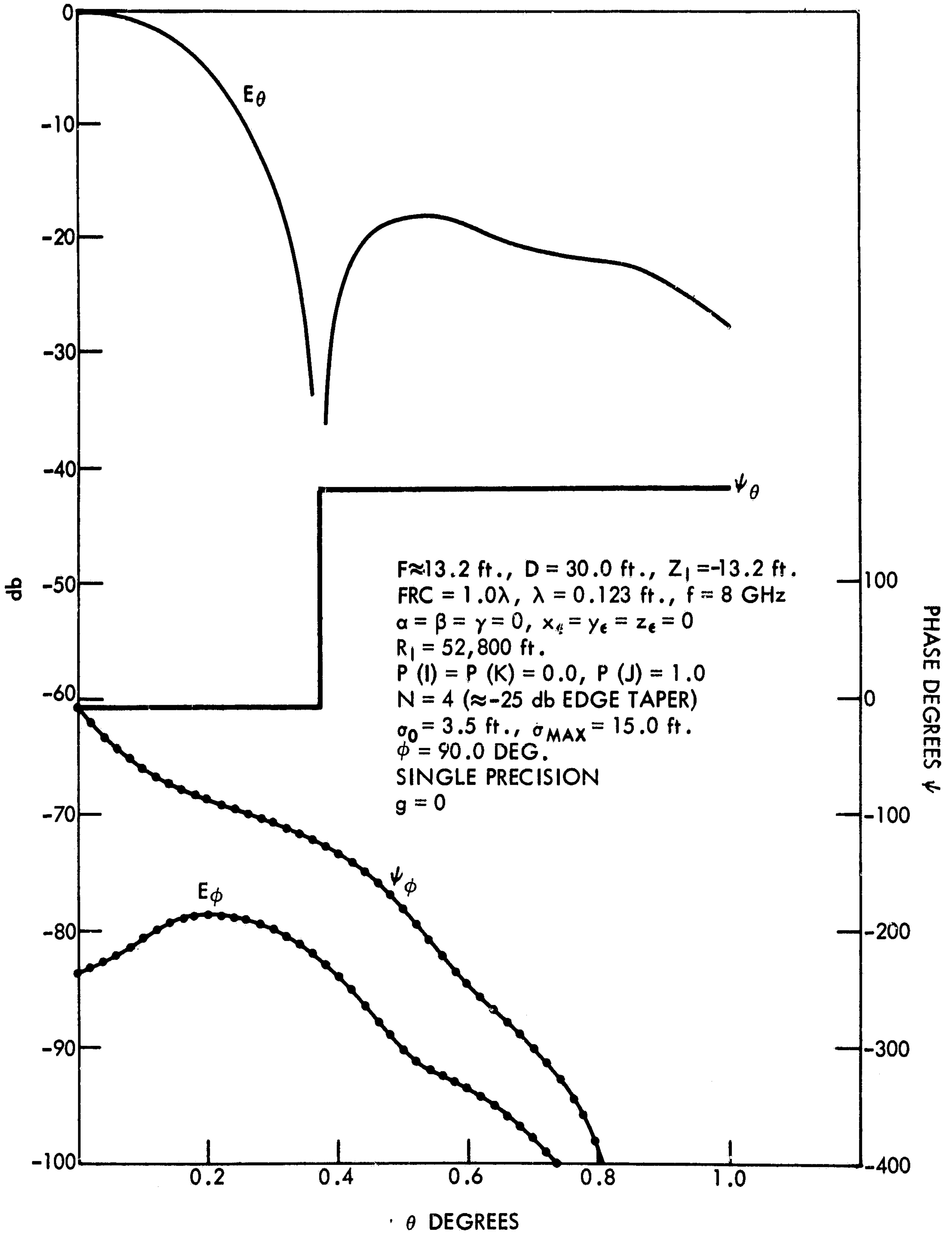

Figure 4–ATS paraboloid without thermal distortion (8 GHz).

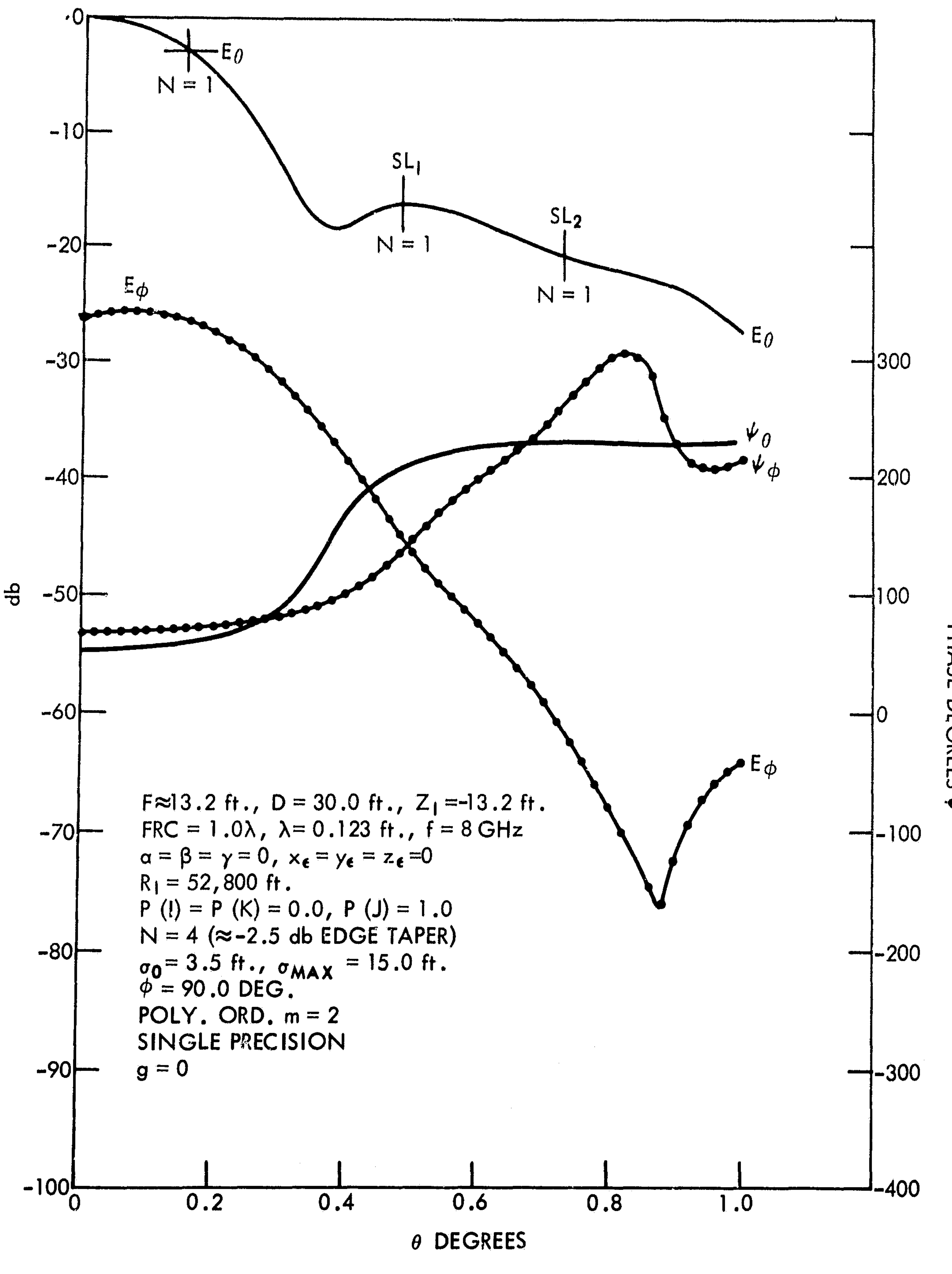

Figure 5–ATS paraboloid with thermal distortion (8 GHz).

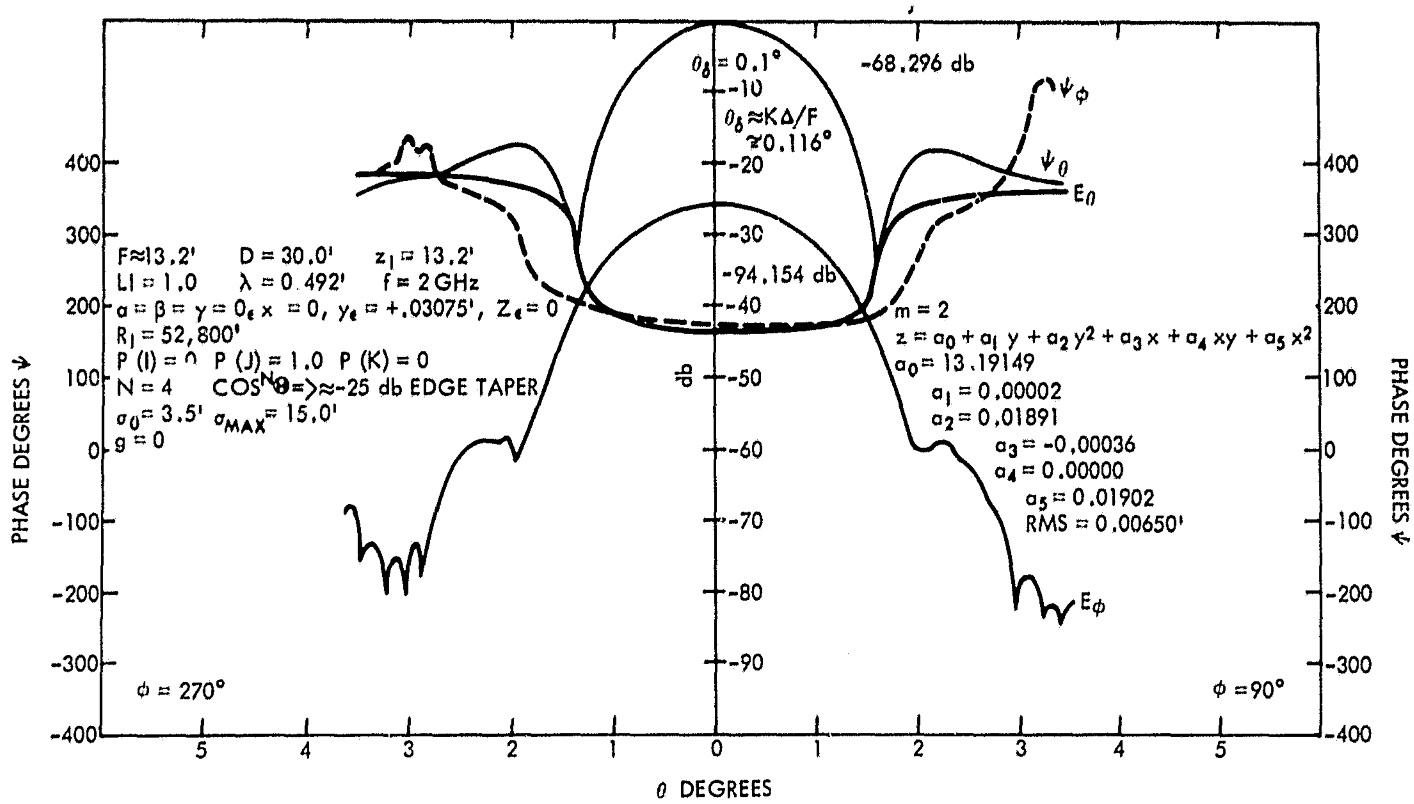

Figure 6–ATS paraboloid with thermal distortion and feed phase-center positioning error (2 GHz).

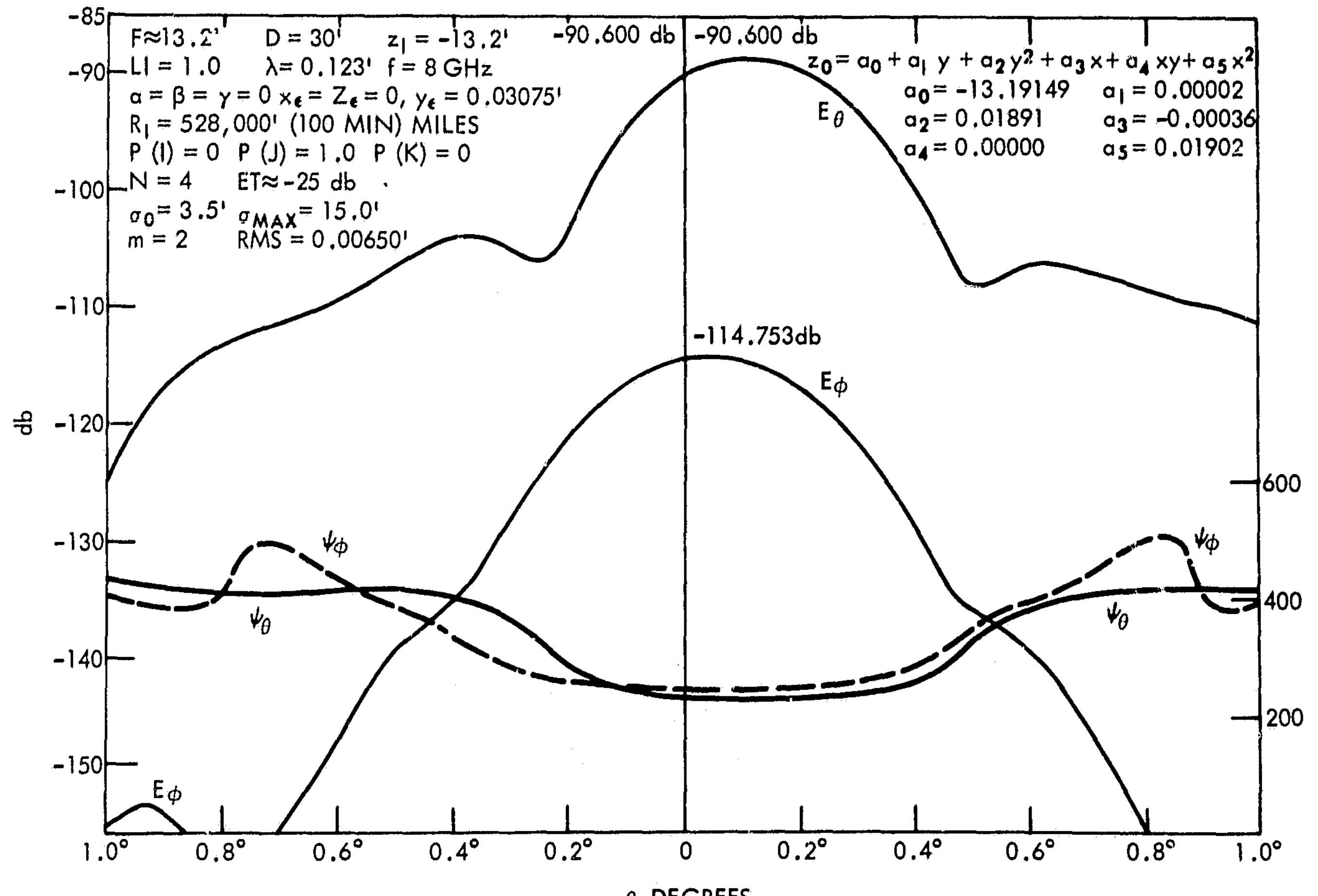

Figure 7–ATS paraboloid with thermal ~~distributor~~ distortion and feed phase-center positioning error (8 GHz).

SUMMARY

The 30-foot ATS reflector was studied at 2 GHz and 8 GHz by means of a computer program based on a vector Kirchhoff formulation. One set of coordinate data (270 degrees past earth-sun line, corresponding to the worst hub-to-tip thermal gradient) was supplied for these computations and extremely serious degradation of the antenna patterns was not observed for the cuts taken here. Prime feed blockage by support structures was not included in this computational investigation, and aperture blockage due to support spars and prime feed was likewise omitted. A subroutine for estimating such second-order effects has been written and tested with the modular program, but was not available for this report.

ACKNOWLEDGMENTS

The author acknowledges the assistance received through many discussions with personnel of the Antenna Systems Branch. Special recognition is also due to: Mr. R. Miezis of Computer Applications, Inc. for programming support, Mssrs. W. Korvin and M. Mills for guidance in determining the ATS antenna parameters, and Mr. G. Honeycutt for supplying the data for the thermally distorted reflector.

REFERENCES

1. Schmidt, R. F., "The Calculation of Antenna Radiation Patterns By A Vector Theory Using Digital Computers" GSFC (X-525-68-201), June 1968.

2. Schmidt, R. F., "The Calculation of Antenna Radiation Patterns By A Vector Theory Using Digital Computers" GSFC (X-525-68-315), August 1968.